Bioorganic & Medicinal Chemistry Letters 19 (2009) 6483–6501

Contents lists available at ScienceDirect

Bioorganic & Medicinal Chemistry Letters

journal homepage: www.elsevier.com/locate/bmcl

Bioorganic & Medicinal Chemistry Letters Volume 19, Issue 23, 2009

Contents

ARTICLES

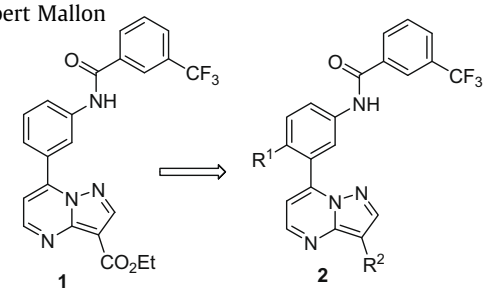

Optimization of initial lead compound **1** provided a series of pyrazolo[1,5-*a*]pyrimidines **2** as potent B-Raf kinase inhibitors.

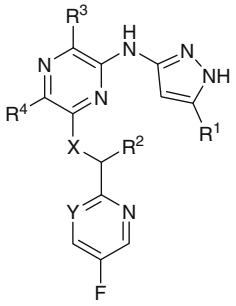

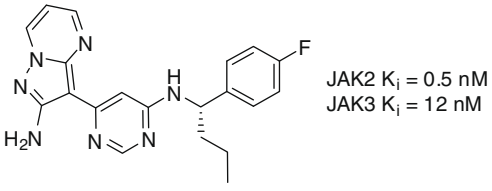

45

The discovery and structure based optimization of a novel series of 2-amino-pyrazolo[1,5-*a*]pyrimidines of potent and selective inhibitors of JAK2 is described.

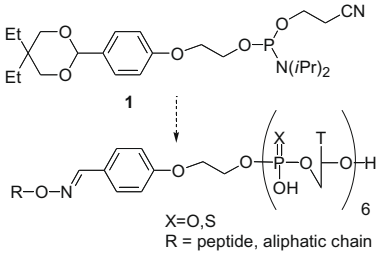

The efficient preparation of oligonucleotide conjugates via the formation of aromatic oxime linkage is reported and is found as efficient as the formation of conjugates through the formation of aliphatic oxime linkage.

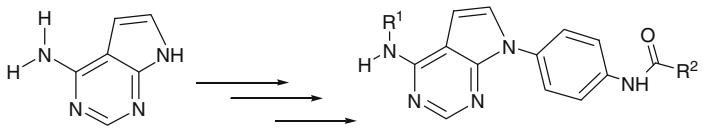

Synthesis of a new series of diarylureas and amides having pyrrolo[2,3-*d*]pyrimidine scaffold is described. Their in vitro antiproliferative activities against A375 human melanoma cell line and HS 27 fibroblast cell line were tested and the effect of substituents on pyrrolo[2,3-*d*]pyrimidine was investigated. The newly synthesized compounds, except *N*-acetyl derivatives (**Id**, **Ie**, and **Im**), generally showed superior or similar activity against A375 to Sorafenib. Among all of these derivatives, compounds **Iq** and **Ir** having imidazole and morpholine moieties, respectively, showed the most potent antiproliferative activity against A375.

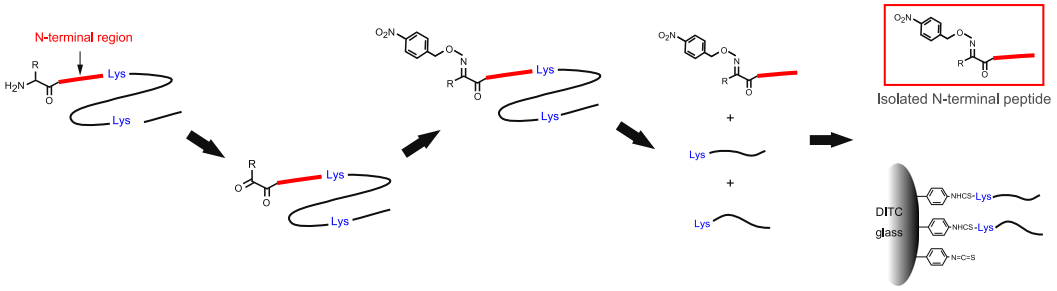

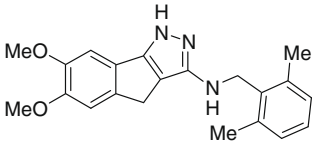

21 (HRI pIC_{50} = 8.1)

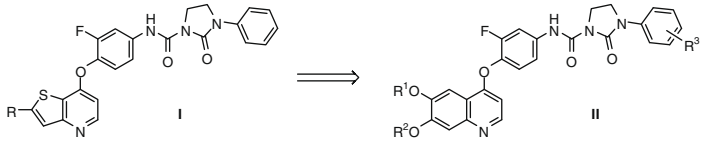

A series of *N*-(4-(6,7-disubstituted quinolin-4-yloxy)-3-fluorophenyl)-2-oxo-3-phenylimidazolidine-1-carboxamides (**II**) targeting c-Met and VEGFR2 tyrosine kinases, based on our previous 2-substituted thieno[3,2-*b*]pyridine series (**I**), was designed and synthesized. The new compounds were potent against these two enzymes with IC_{50} values in the low nanomolar range in vitro, possessed favorable pharmacokinetic profiles and showed high efficacy in vivo in several human tumor xenograft models in mice.

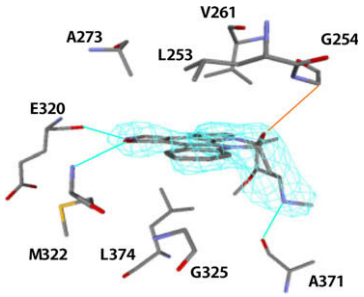

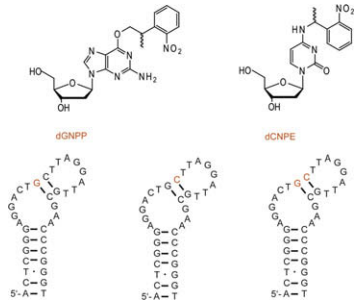

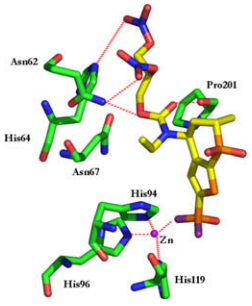

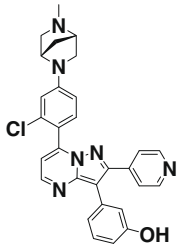

B-Raf enzyme IC_{50} < 0.32 nM
A375 IC_{50} < 10 nM

A series of pyrazolo[1,5-α]pyrimidine analogs has been prepared and found to be extremely potent and selective B-Raf inhibitors.

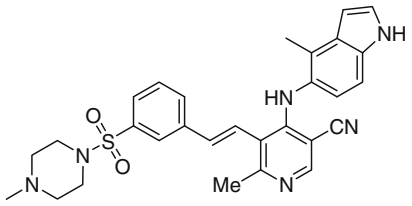

15

A series of vinyl phenyl sulfonamide-3-pyridinecarbonitriles were prepared and evaluated as PKCθ inhibitors. Optimization resulted in the identification of compound **15** with an IC_{50} value of 0.44 nM for the inhibition of PKCθ with 150-fold selectivity over PKCδ.

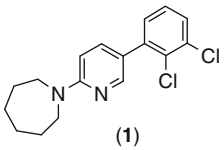

(**1**)

CB_2 pEC_{50} 7.4

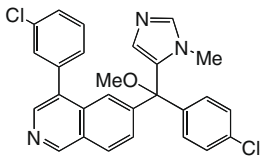

Isoquinoline-based inhibitors of *Trypanosoma cruzi* lanosterol 14a-demethylase are prepared and shown to block the growth of the amastigote life cycle state of the parasite in the sub-nanomolar range.

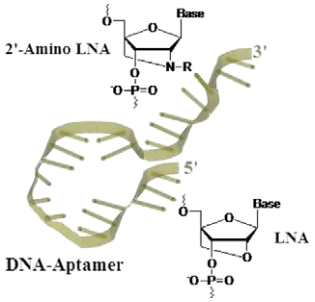

Incorporation of a single LNA modification into an avidin-aptamer confers a significant improvement of affinity, and incorporation of 2′-amino LNA provides options for further derivatisation.

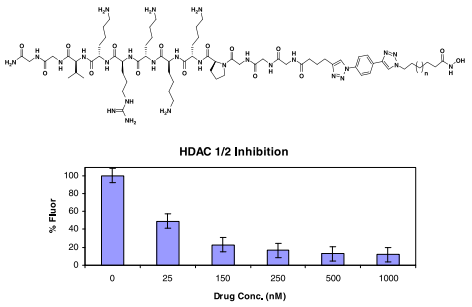

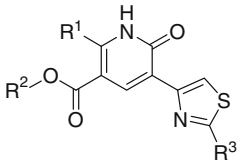

A series of 6-oxo-1,6-dihydropyridines were prepared and found to have potent CDK5 inhibition.

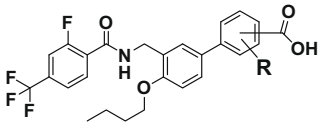

The discovery of new series of PPARδ antagonists are described.

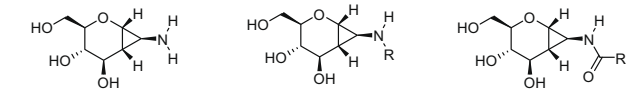

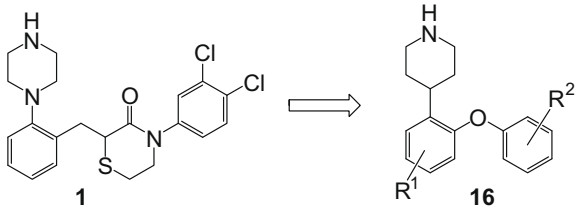

The discovery of piperidine diphenyl ethers (**16**) which combine norepinephrine reuptake inhibition (NRI) with 5-HT1$_A$ partial agonist activity is described. Potent and selective leads were discovered starting from high-throughput screening hits including **1**.

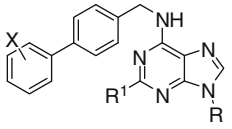

Purines incorporating biarylmethylamino substituents at the C-6 position demonstrated inhibition of cyclin dependent kinases and potent antiproliferative activity.

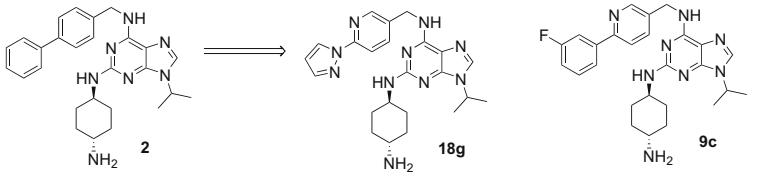

Biaryl purine derivatives such as **2** have demonstrated inhibition of cyclin dependent kinases and potent antiproliferative activity. Replacement of the C-6 biarylmethylamino group with heterobiarylmethylamino groups has afforded compounds such as **18g** and **9c** with significantly improved in vitro activity.

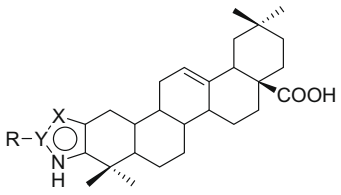

A series of heterocyclic ring-substituted maslinic acid derivatives were prepared and subsequently evaluated on PTP1B, TCPTP and related PTPs in order to increase PTP1B inhibitory activity and especially selectivity for PTP1B over TCPTP.

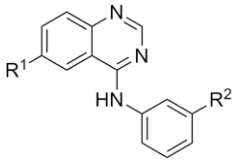

1 R^1 = Br; R^2 = Cl $mGlu_5$ IC_{50} = 256 nM
13 R^1 = Cl; R^2 = Br $mGlu_5$ IC_{50} = 124 nM
32 R^1 = F; R^2 = Br $mGlu_5$ IC_{50} = 96 nM

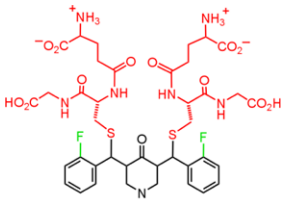

1-$(GSH)_2$

The glutathione conjugates of curcumin analogs represent a promising new series of stable and soluble anti-tumor pro-drugs.

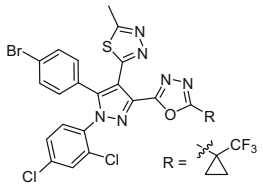

16l
(rCB1 IC_{50} = 1.72 nM)

We have identified novel pentacycles series of small molecule cannabinoid-1 ligands that show potency comparable to that of known rCB1 antagonists. Among various analogues tested, 2-(5-(4-bromophenyl)-1-(2,4-dichlorophenyl)-4-(5-methyl-1,3,4-thiadiazol-2-yl)-1*H*-pyrazol-3-yl)-5-(1-(trifluoromethyl)cyclopropyl)-1,3,4-oxadiazole (**16l**) demonstrated highly favorable binding affinity for rCB1 receptor.

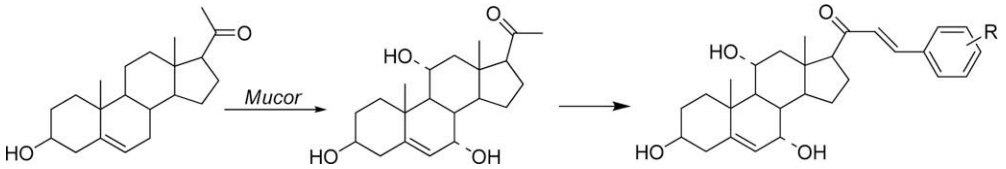

The synthesis and cytotoxic activities evaluation of a series of 3β, 7α, 11α-trihydroxy-pregn-21-benzylidene-5-en-20-one derivatives were described.

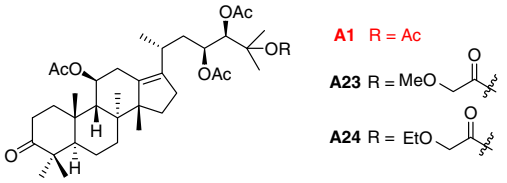

Thirty-two tetra-acylated alisol A derivatives were synthesized and evaluated for their anti-HBV activities and cytotoxicities in vitro. Among them, compounds A1, A23, and A24 exhibited high activities against secretion of HBV surface antigen with IC_{50} values of 0.0048, 0.0044, and 0.014 mM, respectively, HBV e antigen with IC_{50} values of 0.011, 0.012, and 0.018 mM, respectively, and remarkable selective index values of SI_{HBsAg} >333, SI_{HBeAg} >145; SI_{HBsAg} = 209, SI_{HBeAg} = 77; and SI_{HBsAg} >200, SI_{HBeAg} >156, respectively. Additional studies in rats showed that compound A1 has favorable pharmacokinetic prosperities for further development purpose, with elimination half-time ($t_{1/2}$) of 1.63 h and oral bioavailability (F) of 40.9%.

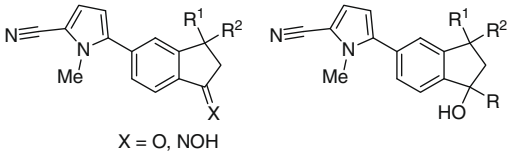

Progesterone receptor agonists and antagonists with low nanomolar in vitro potency are reported.

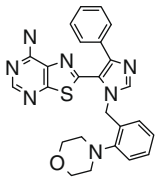

pTie-2 Cell IC_{50} = 440 nM

The SAR and improvement in potency against Tie-2 of novel thienopyrimidine and thiazolopyrimidine kinase inhibitors are reported. These compounds have moderate potency in cellular assays of Tie-2 inhibition, good physical properties, DMPK, and show evidence of in vivo inhibition of Tie-2.

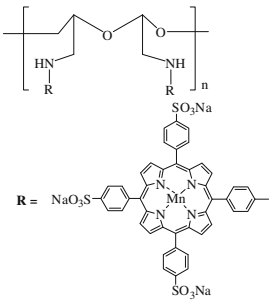

The synthesis and evaluation of Mn porphyrin–dextran as MRI contrast agents are reported.

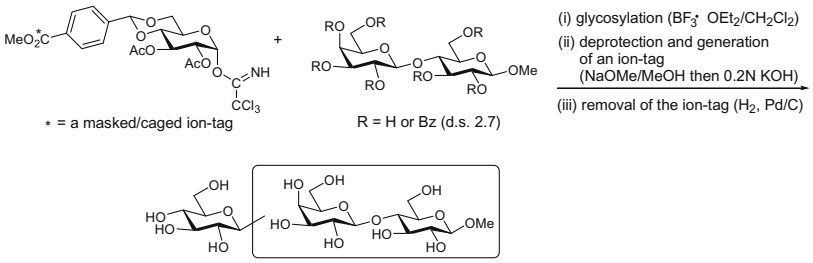

Preparation of oligosaccharide libraries using ionically tagged glycosyl donors.

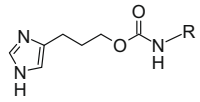

Branched 3-(1*H*-imidazol-4-yl)propyl alkylcarbamates were investigated at the human histamine H_3 receptor (CHO-K1 or HEK-293 cells). A trend for a stereoselectivity at human H_3R was observed for the chiral α-branched ligands. Selected compounds were also tested at the human histamine H_4 receptor (Sf9 cells).

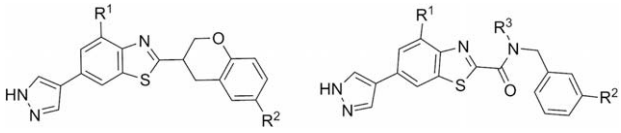

ROCK inhibitors have been developed from 2-chromanyl- and 2-carboxamido-benzothiazoles. SAR studies and lead optimizations are described, which result in novel ROCK-II inhibitors with sub-nanomolar IC_{50}s and good kinase selectivity.

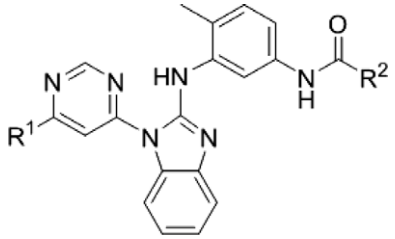

A series of 4-amino-6-benzimidazole-pyrimidines were designed and synthesized as potent Lck inhibitors.

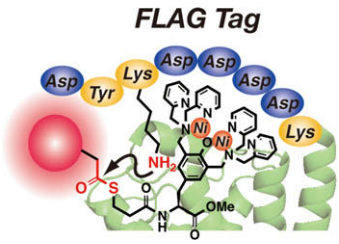

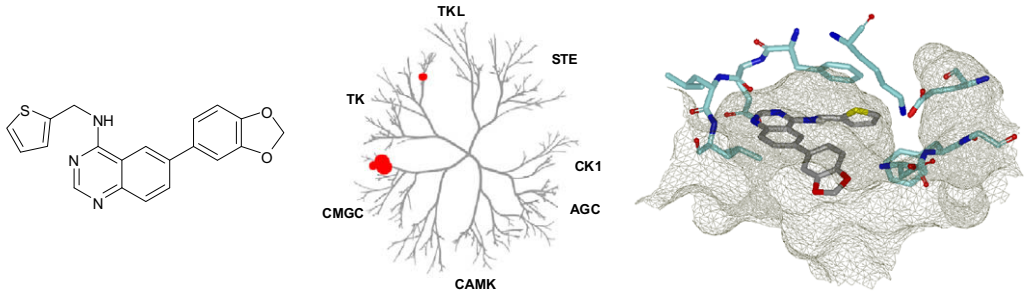

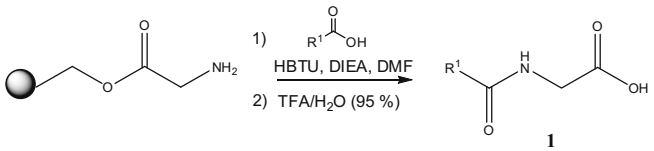

1

The efficient solid phase synthesis of acylglycine human metabolites **1** is reported.

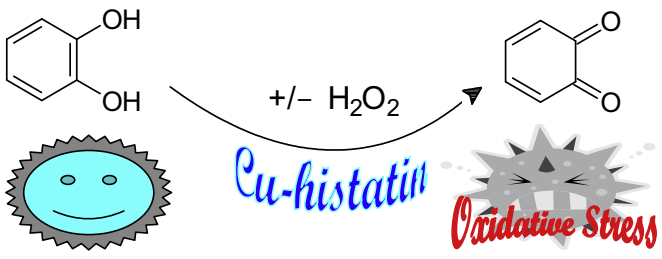

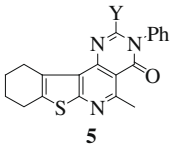

5

The synthesis and biological activity of 2-substituted-8,9,10,11-tetrahydrobenzo[4′,5′]thieno[3′,2′:5,6] pyrido[4,3-*d*]pyrimidin-4(3*H*)-ones **5** are described. The biological evaluation showed that some compounds have antifungal activity against Botrytis cinerea at 50 mg/L and some of them were effective to both KB cells and KBv200 cells.

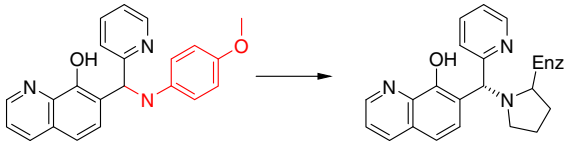

2

Virtual screen hits were shown to be covalent inhibitors by biochemical and X-ray crystallographic studies.

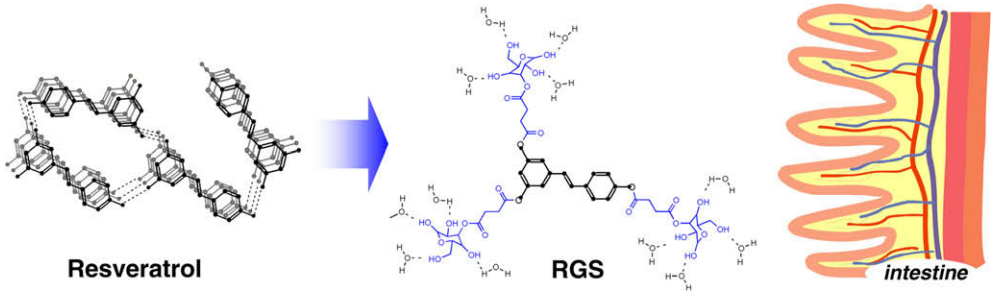

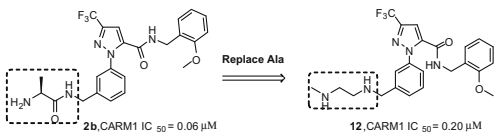

Cpd	N. AUC (PO) μM-h/(mg/Kg)	N. AUC (IV) μM-h/(mg/Kg)	Cl (IV) (L/h)/kg	V_{ss}(IV) L/kg	$t_{1/2}$(IV) hours	% F
2b	0.01	0.04	86	33.6	0.07	-
12	0.07	2.1	1.2	1.4	2.1	4

We have identified the N^1-benzyl-N^2-methylethane-1,2-diamine unit as a substitute for the (*S*)-alanine benzylamide moiety for the design of co-activator associated arginine methyltransferase 1 (CARM1) inhibitors. The potency of these inhibitors is in the same order of magnitude as their predecessors and their clearance, volume of distribution, and half lives were greatly improved.

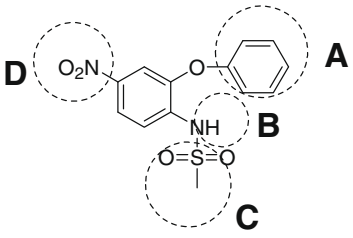

A series of COX-2 selective inhibitor nimesulide derivatives were synthesized as agents to suppress the proliferation of aromatase inhibitor-resistant breast cancer cells.

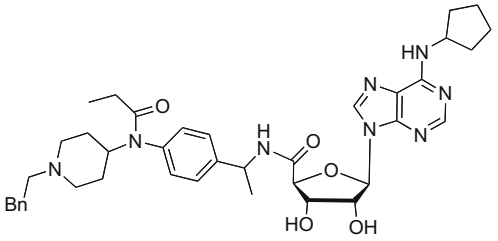

The synthesis and biological activity of a new hetero-bivalent ligand that has antagonist properties on both A_1 adenosine and μ opiate receptors with a K_i of 0.8 ± 0.05 and 0.7 ± 0.03 μM, respectively, are described.

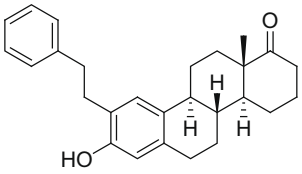

The development of 17β-HSD1 inhibitor (e.g., 2-phenethyl-D-homo-estrone with IC_{50} of 15 nM in vitro) is reported.

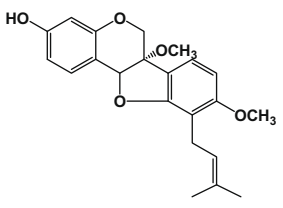

(1)

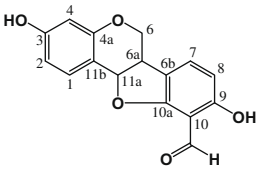

(2)

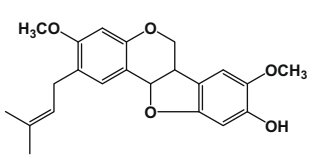

(3)

Three new (**1**–**3**) and 12 known (**4**–**15**) pterocarpan derivatives were isolated from the stem bark of *Erythrina abyssinica* (Leguminosae). All of the isolates were evaluated for their inhibitory effects on protein tyrosine phosphatase-1B (PTP1B), as well as their growth inhibition on MCF-7, MCF-7/TAMR, MCF-7/ADR and MDA-MB-231 breast cancer cell lines.

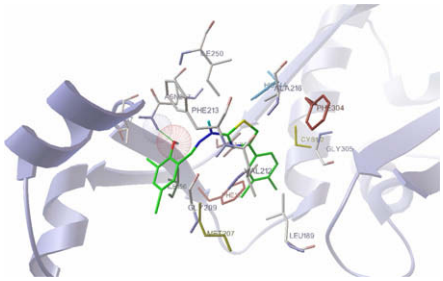

Docking results, along with the data of *Escherichia coli* FabH inhibitory activity assay indicated that compounds **11** and **18** would be potential inhibitors of *E. coli* FabH with potent antibacterial activity.

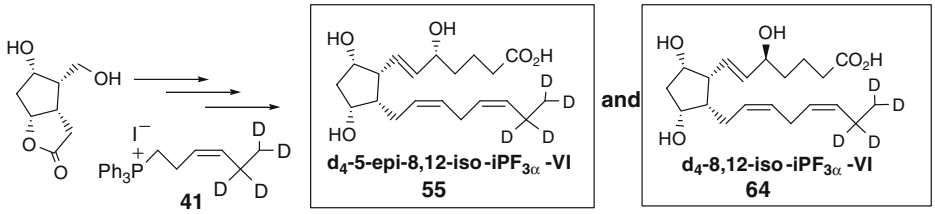

d_4-5-*epi*-8,12-*iso*-$iPF_{3\alpha}$-VI **55** and d_4-8,12-*iso*-$iPF_{3\alpha}$-VI **64** were synthesized using a new strategy to prepare the volatile D_4 synthons. **55** and **64** were subsequently used to quantify iPs in urine.

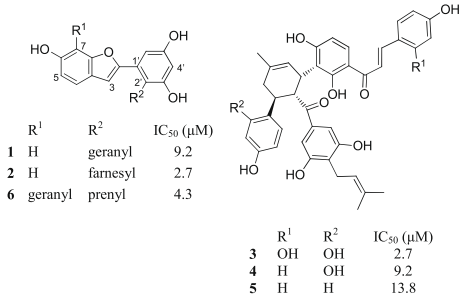

	R^1	R^2	IC_{50} (μM)
1	H	geranyl	9.2
2	H	farnesyl	2.7
6	geranyl	prenyl	4.3

	R^1	R^2	IC_{50} (μM)
3	OH	OH	2.7
4	H	OH	9.2
5	H	H	13.8

Inhibitory constituents against protein tyrosine phosphatase 1B from *Morus bombycis*.

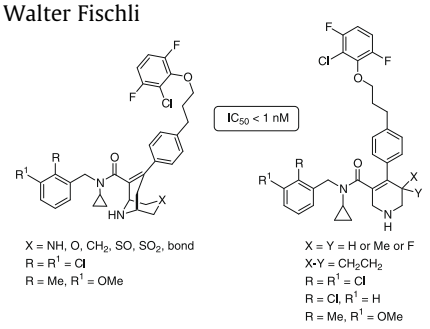

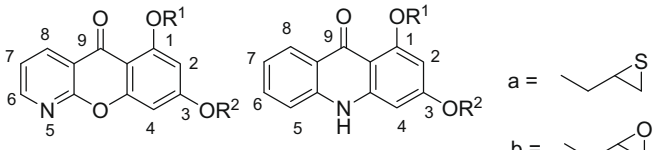

5 R^1 = H, R^2 = a
6 R^1 = a, R^2 = a
7 R^1 = H, R^2 = b
8 R1 = H, R^2 = b
9 R^1 = b, R^2 = b
10 R^1 = H, R^2 = a
11 R^1 = a, R^2 = a

A novel series of isatin-based inhibitors of β-secretase (BACE-1) have been identified using a virtual high-throughput screening approach. Structure–activity relationship studies revealed structural features important for inhibition. Docking studies suggest these inhibitors may bind within the BACE-1 active site through H-bonding interactions involving the catalytic aspartate residues.

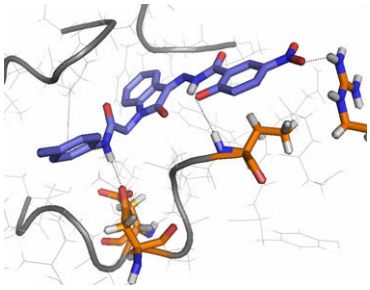

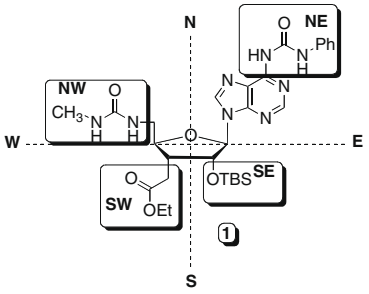

Analogs of lead antiproliferative agent **1** were prepared and tested for activities against the NCI 60 panel of human cancers. Variants in all four canonical quadrants were tested. The 2′-*O*-TBS, 5′-*N*-methylurea, and N^6-phenylurea were necessary for optimal activity.

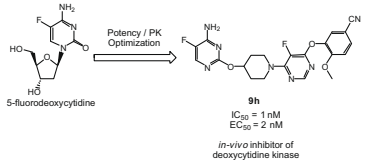

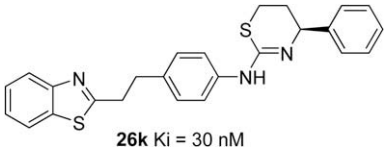

26k Ki = 30 nM

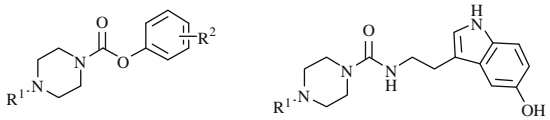

R^1 = 3-chloropyridin-2-yl, 3-trifluoromethylpyridin-2-yl, pyridin-2-ylmethyl, quinolin-2-ylmethyl; R^2 = 4-*t*-Bu, 3-*t*-Bu, 4-CF_3, 3-CF_3, 4-Cl, 3-Cl, 3-Ph

The evaluation of a series of piperazinyl carbamates and ureas, designed on the basis of previously reported TRPV1 antagonists and FAAH inhibitors, led to the identification of some 'dual-action' compounds targeting both FAAH and TRPV1 or TRPA1 channels.

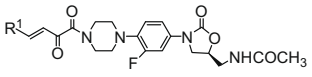

A series of novel oxazolidinone derivatives **3a–j** as potent antibacterial agents is reported. Compound **3f** being the most potent compound of the series having MIC of 0.04–0.19 μg/mL against Gram-positive resistant strains.

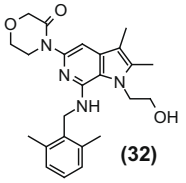

(32)

Parietal cell assay pIC_{50} 7.1
H^+/K^+ ATPase pIC_{50} = 6.6
CHI LogD @ pH 7.4 = 2.93
CYP450 IC50 (μM): 1A2;>100; 2C9,13; 2C19,>100
2D6, 36; 3A4(DEF),6; 3A4(7BQ)11
CLi (ml/min/kg) Rat, 6.5; Human, 6.9

A comparison of in vitro potencies of heterocyclic templates reported as potassium competitive, acid pump antagonists is described. Modification of the more potent 1*H*-pyrrolo[2,3-*c*]pyridine to improve in vitro developability properties leading to compound (**32**) is described.

*Corresponding author
ⓘ+ Supplementary data available via ScienceDirect

COVER

Overlay of high resolution co-crystal structures of *R*-**22**-ADP (cyan) and **1**-ADP (green) bound in an allosteric binding site of the mitotic kinesin KSP. [Roecker, A. J.; Coleman, P. J.; Mercer, S. P.; Schreier, J. D.; Buser, C. A.; Walsh, E. S.; Hamilton, K.; Lobell, R. B.; Tao, W.; Diehl, R. E.; South, V. J.; Davide, J. P.; Kohl, N. E.; Yan, Y.; Kuo, L. C.; Li, C.; Fernandez-Metzler, C.; Mahan, E. A.; Prueksaritanont, T.; Hartman, G. D. *Bioorg. Med. Chem. Lett.* **2007**, *17*, 5677.]

Indexed/Abstracted in: Beilstein, Biochemistry & Biophysics Citation Index, CANCERLIT, Chemical Abstracts, Chemistry Citation Index, Current Awareness in Biological Sciences/BIOBASE, Current Contents: Life Sciences, EMBASE/Excerpta Medica, MEDLINE, PASCAL, Research Alert, Science Citation Index, SciSearch, TOXFILE. Also covered in the abstract and citation database SCOPUS®. Full text available on ScienceDirect®

ELSEVIER

ISSN 0960-894X